DOI: 10.15669/pnst.7.154

*Progress in Nuclear Science and Technology*
Volume 7 (2025) pp. 154-160

**ARTICLE**

# Valence separation of Fe and removal of $Sn^{2+}$ by solvent extraction as a potential method to determine $Fe^{2+}$ in glass containing $Sn^{2+}$

Naoki Kanno [a, b], Masahiko Nakase [a, *], Yoshitaka Saijo [c], Daiju Matsumura [d], Takuya Tsuji [d], Kenji Takeshita [a] and Takehiko Tsukahara [a]

[a] *Laboratory for Zero-Carbon Energy, Tokyo Institute of Technology, N1-2 2-12-1 Ookayama, Meguro-ku, Tokyo 152-8550, Japan;*
[b] *Materials Integration Laboratories, AGC Inc., 1-1 Suehiro-cho, Tsurumi-ku, Yokohama-shi, Kanagawa 230-0045, Japan;*
[c] *Innovative Technology Laboratories, AGC Inc., 1-1 Suehiro-cho, Tsurumi-ku, Yokohama-shi, Kanagawa 230-0045, Japan;*
[d] *Materials Sciences Research Center, Japan Atomic Energy Agency, 1-1-1 Koto, Sayo, Hyogo 679-5148, Japan*

The amounts of $Fe^{2+}$ and $Fe^{3+}$ present in glass are important indicators of its optical properties because even small amounts have significant effects. However, it is challenging to use wet chemical analysis to determine the concentration and the ratio of $Fe^{2+}$ and $Fe^{3+}$ in glass when it contains Sn because of the redox reaction between $Sn^{2+}$ and $Fe^{3+}$ in the glass decomposition solution. A two-step approach was tested to determine the concentrations of $Fe^{2+}$ and $Fe^{3+}$ in a glass decomposition solution in the presence of $Sn^{2+}$. In the first step, the redox reaction between $Sn^{2+}$ and $Fe^{3+}$ was suppressed by increased pH. In the second step, $Sn^{2+}$ was removed from the glass decomposition solution by solvent extraction. To understand the kinetics of the redox reaction between $Sn^{2+}$ and $Fe^{3+}$, time-resolved dispersive X-ray absorption fine structure and ultraviolet-visible absorption spectroscopy (UV-vis) were used with standard chloride solutions of Sn and Fe in respective valences. We found that lowering the acid concentration suppressed redox reactions. The partitioning behaviors of $Sn^{2+}$, $Sn^{4+}$, $Fe^{2+}$, and $Fe^{3+}$ by bis(2-ethylhexyl) hydrogen phosphate (D2EHPA) as an extractant in *n*-dodecane were investigated to see the removal ability of $Sn^{2+}$ from the glass decomposition solution. As a result, D2EHPA in *n*-dodecane could extract $Sn^{2+}$, $Sn^{4+}$, and $Fe^{3+}$ into the organic phase, and $Fe^{2+}$ remained in the aqueous phase. The simultaneous removal of $Sn^{2+}$ and $Sn^{4+}$ and the separation of $Fe^{2+}$ and $Fe^{3+}$ became possible. This method can potentially apply to the rapid analysis of the concentration of $Fe^{2+}$ and $Fe^{3+}$ in a glass containing tin oxide.

***Keywords: Solvent extraction; Extraction-based valence analysis; Redox reaction; Glass; Separation***

## 1. Introduction

Glass is widely used in various industries. Its optical properties are some of the most important properties. The optical properties of the elements in glass determine its optical properties as a whole [1]. One of these elements, iron (Fe), is an important indicator of the optical properties during glass production because even a small amount of Fe ions dramatically affects the optical properties. In addition, $Fe^{2+}$ and $Fe^{3+}$ ions have different optical properties [1]. The concentrations of $Fe^{2+}$ and $Fe^{3+}$ should be evaluated during the glass manufacturing process to maintain consistent optical properties. Both physical and wet chemical analysis methods for determining the concentrations of $Fe^{2+}$ and $Fe^{3+}$ in glass have already been established. Examples of physical analysis methods include X-ray absorption fine structure (XAFS) [2,3] and Mössbauer spectroscopy [4-6]. Examples of wet chemical analysis methods include titration [7] and spectrophotometry [8-11]. Because the concentrations of $Fe^{2+}$ and $Fe^{3+}$ in glass need to be evaluated daily during the glass manufacturing process, wet chemical analysis, which can be performed in a general chemistry laboratory and has a high sensitivity, is mainly used. A representative experimental setup for the decomposition of the glass sample[12] to determine the concentrations of $Fe^{2+}$ and $Fe^{3+}$ in the glass is shown in **Figure S1** (Supplementary Material, SM). Existing methods use reagents degassed in an inert atmosphere to suppress the reaction between Fe ions and oxygen to maintain the valence of ions during decomposition. As previously stated, wet chemical analysis methods for determining the concentrations of $Fe^{2+}$ and $Fe^{3+}$ in glass have already been established. However, these methods make it difficult to suppress the redox reaction of Fe ions with coexisting multivalent elements in glass, such as $Sn^{2+}$.

A small amount of Sn is sometimes added to achieve desired glass properties [13-15]. When glass containing $Fe^{3+}$ and $Sn^{2+}$ is decomposed by acid, a redox reaction between $Fe^{3+}$ and $Sn^{2+}$ proceeds in the decomposed solution at the following standard electrode potentials:

---

*Corresponding author. E-mail: nakase.m.878c@m.isct.ac.jp

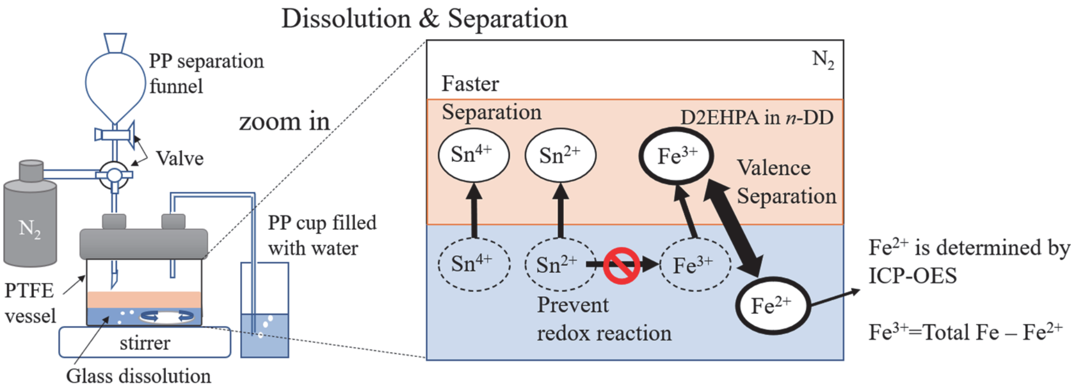

Figure 1. Suppression of redox reaction and separation of $Sn^{2+}$.

$$Sn^{4+} + 2e^- \rightarrow Sn^{2+}\ E^0 = +0.15\ V \quad (1)$$
$$Fe^{3+} + e^- \rightarrow Fe^{2+}\ E^0 = +0.77\ V \quad (2)$$
$$2Fe^{3+} + Sn^{2+} \rightarrow 2Fe^{2+} + Sn^{4+} \quad (3)$$

Therefore, conventional wet chemical analysis methods cannot accurately evaluate the concentrations of $Fe^{2+}$ and $Fe^{3+}$ in glass. Physical analysis methods such as the XAFS and Mössbauer methods are difficult to use in daily analyses at manufacturing sites because they require a radiation-controlled area. In addition, synchrotron radiation used in the XAFS method consumes a large amount of electricity. To rapidly and reliably evaluate the concentrations of $Fe^{2+}$ and $Fe^{3+}$ in Sn-containing glass at a manufacturing site, an energy-saving analytical method that can be performed in a general chemistry laboratory should be established. In this study, fundamental approaches were investigated as to their ability to determine the concentrations of $Fe^{2+}$ and $Fe^{3+}$ in systems containing Sn using conventional wet chemical methods.

The concentrations of $Fe^{2+}$ and $Fe^{3+}$ in a glass decomposition solution in the presence of $Sn^{2+}$ can be determined if $Sn^{2+}$ is removed from the solution before the redox reaction in Eq. (3). Solvent extraction [12,16] and ion exchange are representative methods for separating specific ions from solutions. In this study, a solvent extraction method was developed using bis(2-ethylhexyl) hydrogen phosphate (D2EHPA) in *n*-dodecane, which is an acidic extractant that works well under acidic conditions, with a high extraction efficiency for rare earth elements [17-19]. In general, extraction reactions of metal ions by the D2EHPA are expected as Eq. (4):

$$M^{n+} + nL \Leftrightarrow ML_n + nH^+, (L = D2EHPA) \quad (4)$$

In the case of D2EHPA, the extraction rates of transition metals are lower than those of rare-earth elements [20]. Selective separation of $Sn^{2+}$ from a glass decomposition solution is expected if the extraction efficiency of Sn ions is higher than that of Fe ions. Recent studies have shown that the extraction efficiency of $Fe^{3+}$ is higher than that of $Fe^{2+}$ [21,22]. The concentrations of $Fe^{2+}$ and $Fe^{3+}$ in Sn-containing glasses will be established to determine the concentrations of $Fe^{2+}$ in the glass decomposition solution using inductively coupled plasma optical emission spectroscopy (ICP-OES) after the extraction of $Sn^{2+}$ and $Fe^{3+}$ by D2EHPA in *n*-dodecane.

This study investigated two approaches using a standard solution of Sn and Fe to determine the concentrations of $Fe^{2+}$ and $Fe^{3+}$ in a glass decomposition solution in the presence of $Sn^{2+}$. The first approach was to suppress the redox reaction between $Sn^{2+}$ and $Fe^{3+}$, while the second was to remove $Sn^{2+}$ ions from the glass decomposition solution. Our intent was to apply the existing $Fe^{2+}$ and $Fe^{3+}$ analyses after removing $Sn^{2+}$ from the glass decomposition solution while suppressing the redox reaction. A schematic representation of this approach is shown in **Figure 1**. After investigating the standard behavior for Sn and Fe in this study, these approaches were applied to the glass decomposition vessel shown in **Figure S1** (SM). The parameters that affect the redox reaction rate include acid concentration, temperature, and stirring speed. Since the acid concentration also affects the $Sn^{2+}$ removal efficiency, the redox reaction rates at different acid concentrations were investigated using a standard solution of Sn and Fe. The change of $Fe^{3+}$ concentration after addition of $Sn^{2+}$ to the $Fe^{3+}$ solution was evaluated using ultraviolet-visible absorption spectroscopy (UV-vis). The change of $Sn^{2+}$ concentration after addition of $Fe^{3+}$ to the $Sn^{2+}$ solution was evaluated based on XAFS. In addition, the extraction efficiencies of $Sn^{2+}$, $Sn^{4+}$, $Fe^{2+}$, and $Fe^{3+}$ under HCl conditions by the D2EHPA in *n*-dodecane were investigated using a standard solution of Sn and Fe. The $Fe^{2+}$ and $Fe^{3+}$ extraction behavior in the presence of $Sn^{2+}$ was also investigated using a standard solution of Sn and Fe.

## 2. Experimental

### *2.1. Instruments*

UV-vis (V-750, JASCO Corporation, Tokyo, Japan) and ICP-OES (Agilent5800VDV, Agilent Technologies, Inc., USA) were used. XAFS and time-resolved dispersive XAFS measurements were carried out in the transmission mode at room temperature at BL22XU and BL14B1 of SPring-8, respectively.

### 2.2. Reagents and chemicals

Hydrochloric acid (HCl, 36 mass%) of atomic absorption spectrometry grade, special grade *n*-dodecane (Kanto Chemical Co., Inc., Japan), and bis(2-ethylhexyl) hydrogen phosphate (Tokyo Chemical Industry Co., Ltd., Japan) were used. Standard solutions of Sn and Fe (1 g/L) of ion-chromatography grade (Kanto Chemical Co., Inc., Japan) were used. Special grade tin (II) chloride dihydrate (JUNSEI CHEMICAL Co., Ltd., Japan), tin(IV) chloride pentahydrate (FUJIFILM Wako Pure Chemical Corporation, Japan), iron(II) chloride tetrahydrate (Kanto Chemical Co., Inc., Japan), and special grade iron(III) chloride hexahydrate (JUNSEI CHEMICAL Co., Ltd., Japan) were used. The deionized water was degassed prior to use.

### 2.3. Investigation of the effect of acid concentration on the redox reaction rate of Fe in Fe/Sn mixed solution by UV–vis

Initially, 2.5 mL of 1.0 mmol/L $FeCl_3$ was dissolved in hydrochloric acid (of concentration varying from 0.01 to 1 mol/L) and added to quartz cells. After measuring the background, 1.0 mL of 5.0 mmol/L $SnCl_2$ was dissolved in hydrochloric acid (of concentration varying from 0.01 to 1 mol/L) and quickly added to $FeCl_3$ solutions of equivalent acid concentration. The $Fe^{3+}$ absorbance at 334 nm was measured every second for 1 h at room temperature. The sample solutions were not stirred during measurements. The optical path length of the cell is 1 cm. The conditions of the measured solutions are listed in **Table S1** (SM). The absorbance A was expressed by the Lambert–Beer law of Eq. (5) using the molar absorption coefficient ε, solution concentration c, and optical path length of the cell l. The absorbance and concentration of $Fe^{3+}$ immediately after the addition of the $SnCl_2$ solution were defined as $A_0$ and $c_0$, respectively. $A/A_0$ is expressed as the ratio of $Fe^{3+}$ concentration to the total concentration of Fe using Eq. (6). As the amount of $Sn^{2+}$ added was greater than that of $Fe^{3+}$ required for the redox reaction between $Sn^{2+}$ and $Fe^{3+}$, this reaction was assumed to be a pseudo-first-order reaction of $Fe^{3+}$ ions. The reaction rate constant k for 60 s after adding the $SnCl_2$ solution was calculated from the relationship between $\ln[A/A_0]$ and time t using Eq. (7).

$$\mathrm{A} = \varepsilon \mathrm{cl} \tag{5}$$

$$\frac{\mathrm{A}}{\mathrm{A_0}} = \frac{\varepsilon \mathrm{cl}}{\varepsilon \mathrm{c_0 l}} = \frac{\mathrm{c}}{\mathrm{c_0}} = \frac{\mathrm{Fe^{3+}}}{\mathrm{Total\ Fe}} \tag{6}$$

$$\ln\frac{\mathrm{A}}{\mathrm{A_0}} = -\mathrm{kt} \tag{7}$$

### 2.4. XAFS study of $Sn^{2+}$ and $Sn^{4+}$ in solution

Unlike $Fe^{3+}$, the concentration of $Sn^{2+}$ in an aqueous solution could not be evaluated by UV-vis because $Sn^{2+}$ has weak absorption in aqueous solutions. In this study, the $Sn^{2+}$ concentration was evaluated based on XAFS. XAFS measurements at the Sn K-edge were carried out in transmission mode using a silicon (111) double crystal monochromator at the actinide science II beamline BL22XU of SPring-8. Initially, 1 mL of 10 mmol/L $SnCl_2$ dissolved in 0.1 mol/L HCl was added to a polyethylene bag. X-ray absorption near edge structure (XANES) region and the change of the absorption edge energy of the Sn K-edge in the solution was measured using conventional XAFS. Then, the Sn K-edge in 1 mL of 10 mmol/L $SnCl_4$ dissolved by degassed 0.1 mol/L HCl was measured in the same way.

### 2.5. Time-resolved dispersive XAFS study of relationship between acid concentration and redox reaction rate of Sn in Fe/Sn mixed solution

The $Sn^{2+}$ concentration was evaluated based on the time-resolved dispersive XAFS because the redox reaction proceeded quickly. Time-resolved dispersive XAFS spectra were observed by using following optics. Dispersive XAFS measurements at Sn K-edge were carried out in the transmission mode using a silicon (422) polychromator and complementary metal-oxide semiconductor (CMOS, Hamamatsu photonics) at bending magnet beamline BL14B1 of SPring-8. Initially, 1 mL of 10 mmol/L $SnCl_2$ dissolved in hydrochloric acid adjusted from 0.1 to 1 mol/L was added to quartz cells. Measurement was begun, and after 1 min, an automatic titrator was used to add 0.5 mL of 40 mmol/L $FeCl_3$ dissolved by hydrochloric acid adjusted from 0.1 to 1 mol/L to the $SnCl_2$ solutions, which had the same acid concentrations. XANES region and the change of the absorption edge energy of the Sn K-edge in the solution were measured by dispersive XAFS immediately after adding the $FeCl_3$ solution, where the edge position at the beginning of the measurement was defined as $E_0$. The absorption edge position was evaluated by fitting spectra with an error function and Gaussian function, and it was determined to be a middle point of the step function. The hydrochloric acid concentration was varied to investigate the effect of different acid concentrations on the Sn K-edge position. The Sn K-edge position in the solution was measured for 20 min, and the edge position was defined as $E$. For comparison, the edge position was normalized by the edge position at the beginning of the measurement and the edge position of the $Sn^{4+}$ solution at BL14B1 of SPring-8. The edge position of the $Sn^{4+}$ solution is defined as $E_{4+}$. The normalized edge position (*norm E*) is expressed by Eq. (8). For the $Sn^{2+}$ solution alone, *norm E* is defined as $E_{2+}$. The reaction rate constant, $k$, for 60 s after adding the $FeCl_3$ solution was calculated from the relationship between *norm E* and time $t$ using Eq. (9). The reaction rate constant subtracted from $E_{2+}$ was defined as $k_{sub}$ and was calculated using Eq. (10).

$$norm\ E = \frac{(E-E_0)}{(E_{4+}-E_0)} = \frac{Sn^{4+}}{Total\ Sn} \tag{8}$$

$$ln(1 - norm\ E) = -kt \tag{9}$$

$$ln(1 - (norm\ E - E_{2+})) = -k_{sub}t \tag{10}$$

### 2.6. Investigation of distribution ratios of Sn and Fe ions at several D2EHPA concentrations in n-dodecane

D2EHPA was dissolved in *n*-dodecane in the range of 0.05 - 0.1 mol/L. A 0.1 mol/L hydrochloric acid solution was used to prepare $SnCl_2$, $SnCl_4$, $FeCl_2$, and $FeCl_3$ solutions. Each chloride solution (1.5 mL) was then divided into glass vials. Different concentrations of D2EHPA in *n*-dodecane were added to the vials, and they were shaken at 160 - 170 rpm for 15 min. The aqueous phase was then collected and the concentration of Fe or Sn in the aqueous phase was analyzed using ICP-OES. The distribution ratio of the organic phase to the aqueous phase ($D = org/aq$) was calculated from the difference in the concentration before and after shaking.

### *2.7. Investigation of Sn and Fe extractability by D2EHPA in n-dodecane*

D2EHPA was dissolved in *n*-dodecane to prepare a 100 mmol/L D2EHPA solution. Then, 2 mL of this D2EHPA solution was added to 2 mL of the aqueous solution adjusted to the concentrations listed in **Table S2** (SM) and shaken at 160-170 rpm. The aqueous phase was collected after 5, 15, 30, 45, and 60 min of shaking, and the concentrations of Fe and Sn in the aqueous phase were analyzed using ICP-OES. The extraction rate was calculated from the difference in the concentration before and after shaking, as shown in Eq. (11).

$$percent\ extraction = \frac{(initial\ conc.) - (aq.conc.)}{initial\ conc.} \quad (11)$$

## 3. Results and discussion

### *3.1. Investigation of the relationship between acid concentration and redox reaction rate in $Fe^{3+}/Sn^{2+}$ solution*

**Figure 2 (a)** shows the change in the absorbance of the peak derived from $Fe^{3+}$ in the UV-vis band. The most rapid decrease in the absorbance of $Fe^{3+}$ was observed in the 1.0 mol/L HCl solution, whereas the change in absorbance tended to decrease as the acid concentration was lowered. The reaction rate constants, $k$, calculated as pseudo-first-order reactions, are listed in **Table S3** (SM). A comparison of the reaction rate constants confirmed that the reaction rate decreased significantly with increasing acid concentrations. Therefore, the acid concentration should be decreased to suppress the redox reaction between $Fe^{3+}$ and $Sn^{2+}$.

**Figure S2** (SM) shows the XAFS spectra of $SnCl_2$ and $SnCl_4$ solutions used as references. The Sn K-edge position shifted to a high energy from $Sn^{2+}$ to $Sn^{4+}$, and the ability to identify the valence of Sn using XAFS was confirmed. **Figure S3** (SM) shows the dispersive XAFS spectra of the Sn K edge for 60 s after the addition of the $FeCl_3$ solution to the $SnCl_2$ solution in the case of 1.0 mol/L HCl. The Sn K-edge position shifted to a higher energy over time. **Figure 2 (b)** shows the results of the dispersive XAFS measurements, where the spectra of the Sn K edge position changed over time immediately after the addition of $FeCl_3$ solution to the $SnCl_2$ solution. With an increase in the HCl concentration, the Sn K-edge position shifted to a higher energy for a shorter period. In other words, $Sn^{2+}$ was quickly oxidized to $Sn^{4+}$ with an increase in HCl concentration. The rate of increase in the edge position tended to be suppressed as the acid concentration decreased. It was confirmed that the redox reaction between $Fe^{3+}$ and $Sn^{2+}$ was suppressed as the acid concentration was lowered. This trend in the redox reactions between $Fe^{3+}$ and $Sn^{2+}$ with decreasing acid concentration was consistent with the trend observed in the UV-vis investigation (Figure 2 (a)). However, the oxidation rate of $Sn^{2+}$ appeared to be faster than the reduction rate of $Fe^{3+}$. This was presumably due to differences in the solution conditions and/or air oxidation, as well as the effect of synchrotron radiation. The absorption edge energy gradually shifted to a high value when measured at a hydrochloric acid concentration of 0.1 mol/L without the $FeCl_3$ solution (dashed plot in Figure 2 (b)). This suggests that, in addition to the redox reaction with $Fe^{3+}$, the oxidation of $Sn^{2+}$ by air and synchrotron radiation may have also occurred. **Table S4** (SM) lists the reaction rate constants of $Sn^{2+}$ in solutions containing $Fe^{3+}$. Because the oxidation of $Sn^{2+}$ by air and synchrotron radiation was excluded in the case of $k_{sub}$, $k_{sub}$ was lower than $k$ at the same HCl concentration. **Figure S4** (SM) shows the relationship between HCl concentration and the reaction rate constant for $Sn^{2+}$ in a solution containing $Fe^{3+}$. HCl concentration had a more significant effect on the

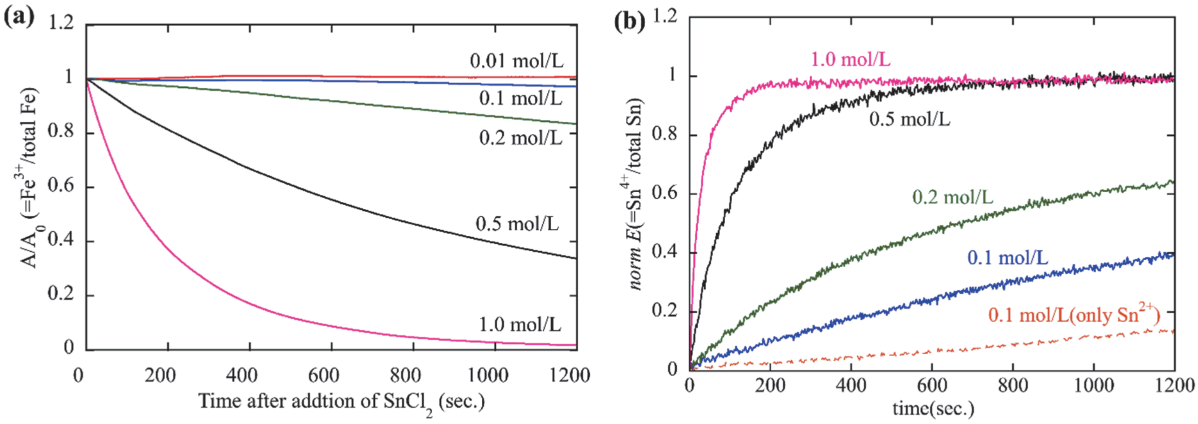

Figure 2. (a) Effect of acid concentration on change over time of $Fe^{3+}$ peak absorbance, (b) Change over time of the Sn K-edge position in the solution determined by dispersive XAFS.

reaction rate than the oxidation of $Sn^{2+}$ by air and/or synchrotron radiation.

These results confirm that the redox reaction between $Fe^{3+}$ and $Sn^{2+}$ proceeded in acidic solutions and could be suppressed by lowering the HCl concentration below 0.1 mol/L. Nevertheless, the redox reaction could not be stopped by lowering the HCl concentration. Therefore, it is desirable to remove $Sn^{2+}$ or separate the valence of Fe, in addition to suppressing the redox reaction by adjusting the acid concentration.

### 3.2. Investigation of extractability of Sn and Fe ions by D2EHPA

The extraction behavior of each ion with D2EHPA was investigated before evaluating the behavior of Sn and Fe mixtures. **Figure 3 (a)** shows the distribution ratios of Sn and Fe ions at different D2EHPA concentrations. The distribution ratio of each Sn ion was higher than that of each Fe ion. $Fe^{2+}$ ions were kept in the aqueous phase under nearly all conditions. These results suggest that only $Fe^{2+}$ ions can be retained in the aqueous phase at the optimal acid concentration and extraction conditions.

**Figure 3 (b)** shows the extraction ratios after shaking for Sn and Fe ions dissolved in HCl, as indicated by Nos. 21 - 24 in Table S2. The extraction rate of $Fe^{2+}$ was low. Figure 3 (a) shows that the extraction capacity of D2EHPA for $Fe^{2+}$ was low. In the solution with $FeCl_3$, almost 100% of $Fe^{3+}$ was extracted by D2EHPA within 5 min after the start of shaking. As for Sn, nearly 100% of the Sn ions were extracted by D2EHPA from both the $SnCl_2$ and $SnCl_4$ solutions within 5 min of shaking. The extraction rate was maintained until 60 min after the start of shaking, suggesting that the extracted Sn was retained in the organic phase. These results confirm that D2EHPA dissolved in *n*-dodecane was very effective at extracting $Fe^{3+}$, $Sn^{2+}$, and $Sn^{4+}$.

The extraction behavior of D2EHPA in the presence of $Fe^{2+}$, $Fe^{3+}$, and $Sn^{2+}$, which undergo redox reactions with $Fe^{3+}$, was confirmed under the conditions shown in Nos. 25 and 26 in Table S2. The results are shown in **Figure 4 (a)** and **4 (b)**. **Figure S5** (SM) shows the extraction rate at 5 min after the start of shaking. The results of the extraction test showed that nearly 100% of $Sn^{2+}$, $Sn^{4+}$, and $Fe^{3+}$ was extracted into the organic phase within 5 min after the start of shaking, and the extraction rates of $Sn^{2+}$, $Sn^{4+}$, and $Fe^{3+}$ remained constant after 5 min of shaking. This suggested that $Sn^{2+}$, $Sn^{4+}$, and $Fe^{3+}$ reached equilibrium 5 min after the start of shaking. When D2EHPA in *n*-dodecane was used, $Fe^{3+}$ was extracted, but $Fe^{2+}$ remained in the aqueous phase, which suggests that this method could also separate $Fe^{2+}$ from $Fe^{3+}$. The $Fe^{2+}$ concentration can be considered as the concentration of Fe remaining in the aqueous phase, as shown in Figure 1. Figure 3 (b) and 4 (a) shows 0-20 % of $Fe^{2+}$ is extracted in

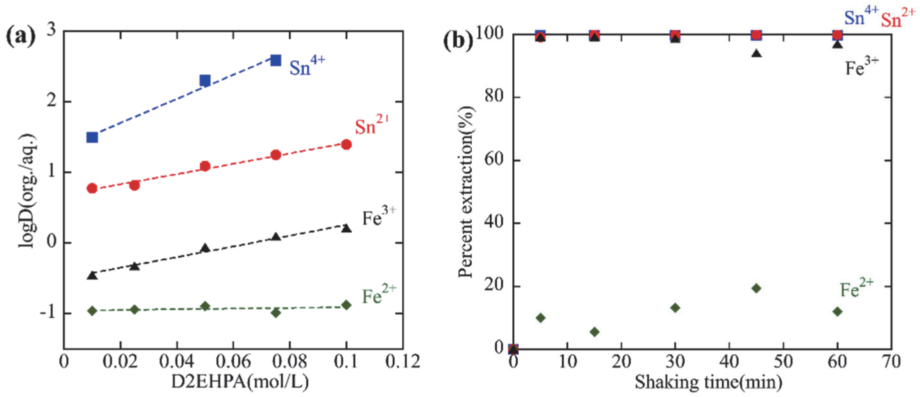

Figure 3. (a) Distribution ratios of Sn and Fe ions at each D2EHPA concentration, (b) Extraction percentage achieved with D2EHPA for each solution.

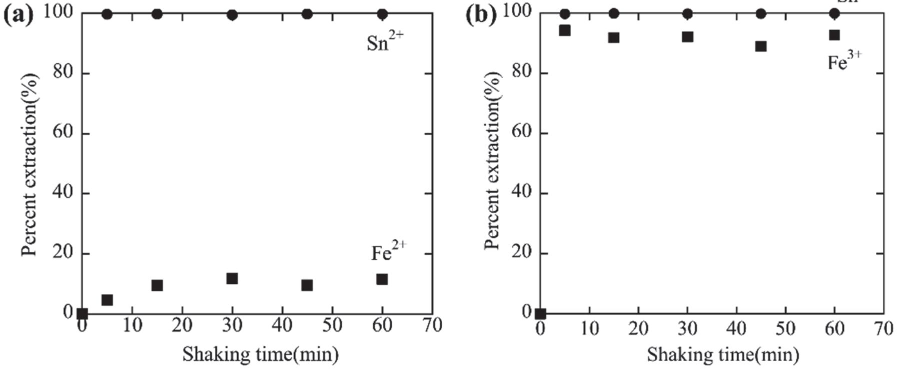

Figure 4. (a) Sn and Fe extraction percentages achieved with D2EHPA in $SnCl_2 + FeCl_2$ solution, (b) Sn and Fe extraction percentages achieved with D2EHPA in $SnCl_2 + FeCl_3$ solution.

the solvent, but an error of 10-15% is considered acceptable; NIST standard glass 1830 has a certified FeO concentration of 0.032 ± 0.004 mass%, which includes an error of 12.5% at the certified value [23]. Since the purpose of the study is to evaluate the valence of Fe in glass daily at the glass manufacturing site, an error of 10-15% is acceptable to prioritize speed.

This investigation was conducted by dissolving the reagents in an aqueous HCl solution; however, the actual glass decomposition solution contains HF and a large amount of glass components. It is necessary to investigate whether a glass analysis solution with a more complicated matrix than that used in this test would exhibit the same extraction ability. As shown in **Figure S6** (SM), in future work we plan to simultaneously perform glass decomposition and $Sn^{2+}$, $Sn^{4+}$, and $Fe^{3+}$ removal using D2EHPA and then analyze the $Fe^{2+}$ in the aqueous phase after separation using ICP-OES to determine the concentration of $Fe^{2+}$. The influence of the glass matrix when applying a glass decomposition solution will be investigated.

## 4. Conclusion

Given that the concentrations of $Fe^{2+}$ and $Fe^{3+}$ in glass need to be evaluated daily during the glass manufacturing process, approaches to regulate the redox reaction between $Fe^{3+}$ and $Sn^{2+}$ in an HCl solution and the extraction kinetics of $Fe^{2+}$, $Fe^{3+}$, $Sn^{2+}$, and $Sn^{4+}$ in an HCl solution were investigated in an attempt to determine the concentration of $Fe^{2+}$ in Sn-containing glasses using conventional wet chemical methods. UV-vis and dispersive XAFS were used to investigate the kinetics of the redox reaction between $Fe^{3+}$ and $Sn^{2+}$, and it was found that the redox reaction could be suppressed by lowering the acid concentration. The partitioning of $Sn^{2+}$, $Sn^{4+}$, $Fe^{2+}$, and $Fe^{3+}$ in D2EHPA in *n*-dodecane was investigated to confirm the conditions under which $Sn^{2+}$ could be extracted into the organic phase. D2EHPA in *n*-dodecane could be used to simultaneously extract $Sn^{2+}$, $Sn^{4+}$, and $Fe^{3+}$ into the organic phase and maintain $Fe^{2+}$ in the aqueous phase. It is thus postulated that the $Fe^{2+}$ concentration can then be analyzed using ICP-OES to determine the Fe concentration in the aqueous phase. The results of this study demonstrate the effectiveness of simultaneously removing $Sn^{2+}$ and $Sn^{4+}$ and separating the Fe valence by reducing the acid concentration to suppress the redox reaction and extraction with D2EHPA in *n*-dodecane. The $Fe^{2+}$ concentration in tin-containing glass could potentially be determined by applying this extraction method during the acid decomposition of glass.

## Acknowledgements

This work was supported by the Nanotechnology Platform (JPMXP09A21AE0033) and the JAEA Advanced Characterization ARIM under the remit of "ARIM" of the Ministry of Education, Culture, Sports, Science and Technology (MEXT), Japan (JPMXP1222AE0004). The conventional XAFS experiments were performed using a JAEA experimental station at BL22XU (2021B-E11), SPring-8, with the approval of JASRI (2021B3739). The time-resolved dispersive XAFS was performed at BL14B1 (2022B-E04), SPring-8 with the approval of JASRI (2022A3625).

## References

[1] T. Kavas, S.J. Alsufyani, Z.A. Alrowaili, N. Tamam, R. Kurtulus, I.O. Olarinoye and M.S. Al-Buriahi, Influence of iron (III) oxide on the optical, mechanical, physical, and radiation shielding properties of sodium-barium-vanadate glass system, *Optik (Stuttg)*. 257 (2022) 168844.

[2] K. Ozawa, K. Hirose and Y. Takahashi, High-pressure XAFS measurements of the coordination environments of $Fe^{2+}$ and $Fe^{3+}$ in basaltic glasses, *J Geophys Res Solid Earth* 127 (2022). https://doi.org/10.1029/2021JB023902.

[3] M. Karabulut, G.K. Marasinghe, C.S. Ray, D.E. Day, G.D. Waddill, C.H. Booth, P.G. Allen, J.J. Bucher, D.L. Caulder and D.K. Shuh, An investigation of the local iron environment in iron phosphate glasses having different Fe(II) concentrations, *J Non Cryst Solids* 306 (2002), pp. 182-192.

[4] J.P. Watt, W. Leiper, J.M. Ade-Hall and D.F. Goble, Measurement of $Fe^{3+}/Fe^{2+}$ ratios in basaltic class I titanomagnetites using the Mössbauer effect, *J Geophys Res.* 78 (1973), pp. 3301-3309.

[5] K.F.E. Williams, C.E. Johnson, J. Greengrass, B.P. Tilley, D. Gelder and J.A. Johnson, Tin oxidation state, depth profiles of $Sn^{2+}$ and $Sn^{4+}$ and oxygen diffusivity in float glass by Mössbauer spectroscopy, *J Non Cryst Solids.* 211 (1997), pp. 164-172.

[6] D.G. Karraker, Ferrous/ferric ratio in DWPF glass: Chemical and sup 57 Fe Moessbauer determinations, *Adv Ceram Mater*. (USA). 3 (1988), pp. 337-340.

[7] W.D. Johnston, Oxidation-reduction equilibria in iron-containing glass, *Journal of the American Ceramic Society*. 47 (1964), pp. 198-201.

[8] D.R. Jones, W.C. Jansheskl and D.S. Goldman, Spectrophotometric determination of reduced and total iron in glass with 1,10-phenanthroline, *Anal Chem*. 53 (1981), pp. 923-924.

[9] J.E. Amonette and J. Matyáš, Determination of ferrous and total iron in refractory spinels, *Anal Chim Acta*. 910 (2016), pp. 25-35.

[10] E.W. Baumann, Colorimetric determination of iron(II) and iron(III) in glass, *Analyst*. 117 (1992), pp. 913-916.

[11] O. Corumluoglu and E. Guadagnino, Determination of ferrous iron and total iron in glass by a colorimetric method. Report of ICG/TC2, 'Chemical Durability and Analysis,' *Glass Technol*. 40 (1999), pp. 24-28.

[12] Y. Saijo, M. Murata, T. Kajihara, H. Hijiya, Y. Suzuki, R. Akiyama, M. Shimizu, Y. Shimotsuma and K. Miura, Speciation of tin ions in oxide glass containing iron oxide through solvent extraction and inductively coupled plasma atomic emission spectrometry after the decomposition utilizing ascorbic acid, *Anal Sci*. 38 (2022), pp. 881-888.

[13] J.D. Musgraves, J. Hu and L. Calvez, *Springer*

*Handbook of Glass*, (2019), p. 1851.

[14] A. Ellison and I.A. Cornejo, Glass substrates for liquid crystal displays, *Int J Appl Glass Sci*. 1 (2010), pp. 87-103.

[15] K. Kim, Fining behavior in alkaline earth aluminoborosilicate melts doped with As2O5 and SnO2, *J Am Ceram Soc*. 96 (2013), pp. 781-786.

[16] Y. Saijo, Y. Suzuki, R. Akiyama, M. Shimizu, Y. Shimotsuma and K. Miura, Speciation analysis of tin at the tin side of float glass by solvent extraction combined with a stepwise etching technique, *J Non Cryst Solids*. 592 (2022), p. 121752.

[17] R.D. Abreu and C.A. Morais, Study on separation of heavy rare earth elements by solvent extraction with organophosphorus acids and amine reagents, *Miner Eng*. 61 (2014), pp. 82-87.

[18] M. Nascimento, B.M. Valverde, F.A. Ferreira, R.D.C. Gomes and P.S.M. Soares, Separation of rare earths by solvent extraction using DEHPA, *Rem: Revista Escola de Minas*. 68 (2015), pp. 427-434.

[19] H. Chang, M. Li, Z. Liu, Y. Hu and F. Zhang, Study on separation of rare earth elements in complex system, *J Rare Earths*. 28 (2010), pp. 116-119.

[20] Y. Zhang, F. Gu, Z. Su, S. Liu, C. Anderson and T. Jiang, Hydrometallurgical recovery of rare earth elements from NdFeB permanent magnet scrap: A review, *Met*. 10 (2020) p. 841.

[21] G. Hu, Y. Wu, D. Chen, Y. Wang, T. Qi and L. Wang, Selective removal of iron(III) from highly salted chloride acidic solutions by solvent extraction using di(2-ethylhexyl) phosphate, *Front Chem Sci Eng*. 15 (2020), pp. 528-537.

[22] Y. Jin, Y. Ma, Y. Weng, X. Jia and J. Li, Solvent extraction of $Fe^{3+}$ from the hydrochloric acid route phosphoric acid by D2EHPA in kerosene, *J Ind Eng Chem*. 20 (2014), pp. 3446-3452.

[23] National Institute of Standards & Technology, Certificate of Analysis, Standard Reference Material® 1830, Certificate/Report (2017).